Roles for β-Catenin and Doxycycline in the Regulation of Respiratory Epithelial Cell Frequency and Function

Russell W. Smith[1], Douglas A. Hicks[1], and Susan D. Reynolds[1]

[1]Department of Pediatrics, National Jewish Health, Denver, Colorado

The expression of β-catenin–dependent genes can be increased through the Cre recombinase (Cre)–mediated elimination of the exon 3–encoded sequence. This mutant β-catenin is termed DE3, and promotes the expression of β-catenin–dependent genes. Our previous study used the DE3 model to demonstrate that persistent β-catenin activity inhibited bronchiolar Clara-to-ciliated cell differentiation. The present study was designed to evaluate the roles of β-catenin in regulating the tracheal progenitor cell hierarchy. However, initial experiments demonstrated that the tetracycline-responsive element–Cre transgene (TRE-Cre) was active in the absence of a reverse tetracycline transactivator driver or inducer, doxycycline (Dox). This spurious TRE-Cre transgene activity was not detected using the ROSA26-floxed STOP-LacZ reporter. To determine if the phenotype was a consequence of genotype or treatment with Dox, tracheal and lung specimens were evaluated using quantitative histomorphometric techniques. Analyses of uninduced mice demonstrated a significant effect of genotype on tracheal epithelial cell mass, involving basal, Clara-like cell types. The bronchial and bronchiolar Clara cell mass was also decreased. Paradoxically, an effect on ciliated cell mass was not detected. Activation of the β-catenin reporter transgene TOPGal demonstrated that β-catenin–dependent gene expression led to the genotype-dependent tracheal and bronchiolar phenotype. Comparative analyses of wild-type or keratin 14-rtTA$^{+/0}$/TRE-cre$^{+/0}$/DE3$^{+/+}$ mice receiving standard or Dox chow demonstrated an effect of treatment with Dox on basal, Clara-like, and Clara cell masses. We discuss these results in terms of cautionary notes and with regard to alterations of progenitor cell hierarchies in response to low-level injury.

Keywords: Clara cell; doxycycline; Cre recombinase; β-catenin; stereology

LUNG EPITHELIAL CELL LINEAGES

The tracheobronchial, bronchiolar, and alveolar compartments of murine airway epithelia contain distinct cell lineages. Within the tracheobronchial compartment, basal cells act as progenitors of secretory and ciliated cells during lung development (1). However, Clara-like cells are the progenitors of ciliated cells in the adult steady-state trachea (2). After treatment with naphthalene (NA), the basal cell becomes the progenitor of nascent Clara-like and ciliated cells (3–7). We suggested that signaling from Clara-like cells to basal cells limits the fate of adult basal cells to self-renewal (3).

CLINICAL RELEVANCE

We demonstrate that the tetracycline-responsive element–Cre transgene functions independently of a driver and of doxycycline in some settings. In the context of a floxed β-catenin allele, this spurious activity alters differentiated cell masses in tracheal, bronchial, and terminal bronchiolar epithelia. We discuss these results in cautionary terms and in regard to alterations of progenitor cell hierarchies in response to low-level injury.

The bronchiolar epithelium is maintained by Clara cells (8, 9), whereas the alveolar epithelium is maintained by Type II cells (10). Tracing the lineage of bronchiolar Clara cells demonstrated that the airway and alveolar epithelia comprise distinct lineages in the steady state (11). Although injury may lead to bronchiolarization of the alveolar duct or alveolarization of the terminal bronchiole (12–14), the roles for a dual-lineage cell, termed the bronchoalveolar stem cell, (13) have been challenged (9, 15). The molecular mechanisms that establish these lineages have received intense scrutiny, and β-catenin was identified as one player in this process.

FUNCTIONS OF β-CATENIN IN LUNG DEVELOPMENT

The WNT/β-catenin signaling pathway is active during endodermal development, and is down-regulated during the pseudoglandular-to-alveolar transition (11, 16–18). Studies by several groups established the principle that endoderm specification requires a precise regulation of β-catenin–dependent genes (17, 19, 20). This principle is consistent with results from other organ systems indicating that too little or too much β-catenin–dependent gene expression altered the specification of cellular fates, phenotypic maturation, and tissue repair, as reviewed by De Langhe and Reynolds (18).

β-CATENIN STABILIZATION ALLELE

The function of β-catenin–dependent genes in respiratory epithelial differentiation was evaluated by the extension or reactivation of β-catenin–dependent gene expression. This system uses the Cre recombinase–mediated excision of β-catenin exon 3 (the DE3 allele) (21), and results in the generation of a transcriptionally active β-catenin protein that lacks the GSK3 phosphorylation sites (21). This mutant β-catenin (DE3) is "stabilized" relative to wild-type (WT) β-catenin, and results in the increased expression of β-catenin–dependent genes.

DOXYCYCLINE-REGULATED SYSTEM

Several genetic systems were used to recombine the DE3 allele. Among these, the doxycycline (Dox)–regulated system allows for temporal control of the recombination event and for cellular specificity. This system is regulated by a driver transgene, composed of a cell-type–specific promoter and a reverse-tetracycline transactivator (rtTA). Sensitivity to Dox is conferred by the

tetracycline-responsive element (TRE) transgene, which expresses Cre recombinase. Experiments involving the Dox system are controlled using monotransgenic and bitransgenic mice that are negative or positive for the floxed allele, and test groups that receive standard or Dox chow. Generally, rtTA transgenes are well tolerated (22), although some toxic effects were reported (23, 24). Similarly, the TRE-Cre transgene is typically benign, although some effects were reported in the absence of a floxed allele (24). This effect may be attributable to the toxicity of Cre recombinase itself (25).

β-CATENIN–DEPENDENT EPITHELIAL PHENOTYPE

Both the Dox-regulated system and simple cell type–specific promoter–Cre transgenes were used to determine the role played by β-catenin in epithelial differentiation. The surfactant protein C-rtTA and TRE-Cre transgenes were used to demonstrate β-catenin–dependent airway epithelial squamation, mucuscell metaplasia, and simplification of the alveolar compartment (26). A high frequency of mice exposed to Dox during gestation developed adenocarcinoma as adults. Li and colleagues (27) stabilized β-catenin early in lung epithelial development (approximately embryonic days post coitus [edc] 9.5), using the Nkx2.1–Cre transgene and the DE3 allele. They demonstrated the formation of polyps in the trachea and upper airways. The polyps were devoid of ciliated and Clara-like cells, suggesting that excess β-catenin blocked the generation of the tracheal secretory/ciliated lineage. However, the specific progenitor/progeny relationship altered by DE3 was unclear.

In contrast with the phenotype associated with the very early stabilization of β-catenin, genetic modifications during the pseudoglandular phase of lung development (approximately edc 15.5) were less severe (11). Using the Clara cell secretory protein (CCSP)–Cre transgene and the DE3 allele, we demonstrated that stabilization of β-catenin attenuated the postnatal maturation of bronchiolar Clara cells. The stabilization of β-catenin did not alter proliferation of Clara cells in the steady state or in response to NA injury. However, this modification did block Clara-to-ciliated cell differentiation. Collectively, studies of β-catenin stabilization indicated that the attenuation of β-catenin–dependent gene expression plays an important role in determining the fate of Clara cells.

STEREOLOGICAL ANALYSIS OF AIRWAY EPITHELIA

Changes in the conducting airway epithelia are evaluated using quantitative techniques (4, 11, 28, 29). The "traditional method" determines the frequency of a cell type as a function of the length of the basement membrane. This method is valid if the nuclear or cellular volume is constant between comparison groups. Stereological methods (30) can be used to evaluate this bias or to avoid the issue entirely. Here, we used stereological methods to determine whether the total mass of various cell types differed according to genotype or treatment.

Stereological methods do not determine numbers of objects. Rather, the volume density of an object (V_v) is presented as a function of a surface density (S_v). Thus, the thickness of an epithelium or the volume of a specific cell type per area of the basement membrane is presented as V_v/S_v. This term is referred to as "total cell mass" (31), and involves units of $\mu m^3/\mu m^2$. Volume densities (V_V) of various cell types were determined by the point counting of tracheal epithelial profiles. The reference space for this evaluation was the epithelium. V_V is presented in $\mu m^3/\mu m^3$, but is in reality a unitless term. The surface density of the basement membrane (S_V) can be determined by point and intercept counting. The reference volume was the epithelium.

STUDY RATIONALE AND DESIGN

The initial goal of this study was to determine the role of β-catenin–dependent genes in regulation of reparative tracheal basal cells. We previously demonstrated that all reparative basal cells expressed keratin (K) 14 (32). Thus, we planned to use the K14-rtTA$^{+/0}$/TRE-Cre$^{+/0}$/DE3$^{+/+}$ (BiTg) model to stabilize β-catenin in reparative cells. We had also shown that K14$^+$ cells comprised less than 1% of bronchial epithelial cells, and that K14$^+$ cells were absent from the bronchiolar epithelium (4). Consequently, a steady-state phenotype was not expected in a system regulated by the K14 promoter. Despite this rationale, histological alterations were detected in steady-state bronchial and bronchiolar epithelia from BiTg mice that received Dox chow for 19 days (between ages 4 and 7 weeks). Identification of this unexpected phenotype in a basal cell–deficient epithelial region led us to determine the frequency of basal, Clara-like, Clara, and ciliated cells in the BiTg murine strain, and to determine if changes in these frequencies were dependent on (*1*) genotype or (*2*) treatment (i.e., exposure to Dox).

MATERIALS AND METHODS

Additional details are provided in the online supplement.

Animals

All animal studies were reviewed and approved by the Institutional Animal Care and Use Committee of National Jewish Health. Adult (8–14 weeks old) male mice were used for all experiments. We used five alleles: K14rtTA (33), TRE-Cre (34), β-catenin floxed exon 3 (DE3) (21), ROSA26-floxed STOP-LacZ (35), and TOPGal (C57Bl/6 congenic) (36). Mice were bred to generate various combinations of alleles as well as monotransgenic and bitransgenic controls.

Exposures to Dox

On Day 0, animals were placed on Dox chow (625 mg/kg; Harlan, Indianapolis, IN), and switched to standard chow on Day 6 or 19. Animals were killed on either Day 6 or 19. Control mice received standard chow.

Histology

Animals were killed by an injection of 17.5 mg 2,2,2-tribromoethanol in tert-amyl alcohol (intraperitoneal), followed by exsanguination. Trachea/esophagus and lung units were instilled with 10% neutral buffered formalin at 10 cm of water pressure for 10 minutes. The tissue was removed and immersion-fixed in 10% neutral buffered formalin for 2 hours at room temperature.

Staining for β-galactosidase (β-gal) was performed using a staining solution containing an X-galactosidase (X-gal) concentration of 1 mg/ml (36). Whole tissue units were incubated in the staining solution for 3 hours at 37°C. Stained tissues were sectioned and counterstained with Nuclear Fast Red (Vector Laboratories, Burlingame, CA) and coverslipped with Permount (Sigma Chemical Co., St. Louis, MO).

For immunofluorescence staining, tissue sections (5 μm) were generated from paraffin-embedded tissue, cleared with xylene, and rehydrated using a graded ethanol series. All antibodies and methods were previously described (32), with the exception of the rabbit–anti-Cre recombinase (EMD 4Biosciences, Darmstadt, Germany). Images were acquired using a Zeiss Imager.Z1 fluorescent microscope (Carl Zeiss AG, Oberkischen, Germany) equipped with Zeiss Plan-APOCHROMAT ×20/0.8 (Zeiss) and EC Plan-NEOFLUAR ×40/0.75 lenses (Zeiss) and an Axiocam HRm black-and-white digital camera (Zeiss), using AxioVision release 4.6.3 SP1 software (Zeiss).

Morphometry

The total cell masses (V_v/S_v) of various epithelial cell types in tracheal, bronchial, and terminal bronchiolar epithelia were analyzed according to morphometric methods (30, 31, 37). The regions of tracheal analyses

were randomly selected from the cartilaginous (ventral) aspect, and included tracheal rings 4–10. Bronchial regions were defined by the presence of muscle. Terminal bronchiolar regions were defined as previously stated (28). Regions were imaged at ×200 magnification, and each image encompassed approximately 400 μm of the basement membrane. Three to four images were evaluated for groups of three mice per genotype.

Western Blots

Tissues were homogenized in radioimmunoprecipitation assay buffer on ice, centrifuged at $10,000 \times g$, and the supernatants were collected. Samples were separated using precast 4–12% Bis-Tris gels, and were transferred to polyvinylidene fluoride membranes, using a BioRad Criterion system (Bio-Rad, Hercules, CA). Membranes were blocked overnight at 4°C in Odyssey blocking buffer (Li-Cor Biosciences, Lincoln, NE). Primary antibodies were incubated overnight at 4°C. Secondary antibodies were applied for 1 hour at room temperature. Membranes were washed and scanned on a Li-Cor Odyssey Imager (Li-Cor). Primary antibodies included murine monoclonal anti-actin (C-2) (Santa Cruz Biotechnology, Santa Cruz, CA), rabbit anti–β-catenin (N-terminal; Cell Signaling Technology, Danvers, MA), and murine anti–β-catenin (C-terminal; BD Biosciences, Mississauga, ON, Canada). Secondary antibodies included goat anti-mouse infrared (IR) and goat anti-rabbit infrared (IR) 680 (Li-Cor).

Statistical Analysis

The statistical analysis used *t* tests and two-way ANOVA, with *post hoc* Bonferroni analysis.

RESULTS

Initial Characterization of the BiTg Model

We previously demonstrated that K14-expressing basal cells comprised 20% of the steady-state tracheal basal-cell population (32), less than 1% of bronchial epithelial cells, and were absent from bronchiolar epithelia (4). Consequently, a phenotype was not anticipated in a system regulated by K14 promoter (BiTg) mice. Despite this rationale, histological analyses of bronchial and bronchiolar epithelia from BiTg mice that received Dox chow for 19 days (from 4–7 weeks of age) detected cells that were unusually large and highly autofluorescent, and that expressed CCSP (Figure 1). The identification of this unexpected phenotype in a basal cell–deficient epithelial region led us to determine the frequency of basal, Clara-like, Clara, and ciliated cells in this murine strain, and to determine if changes in these frequencies were dependent on (*1*) genotype or (*2*) treatment (i.e., exposure to Dox).

Effects of Genotype on the Total Mass (Vv/Sv) of Differentiated Tracheal Cell Types

Histological analysis of the trachea. To determine the impact of genotype on cellular phenotype, normal adult male mice received standard chow. The test groups included (*1*) WT transgene-negative (rtTA$^-$/Cre$^-$), (*2*) rtTA$^+$ (K14-rtTA$^+$/TRE-Cre$^-$), (*3*) Cre$^+$ (K14-rtTA$^-$/TRE-Cre$^+$), and (*4*) BiTg (K14-rtTA$^+$/TRE-Cre$^+$). All mice were homozygous for the Catnb^{fExon3} (DE3) allele.

Dual immunofluorescence analysis of K5 and K14 demonstrated a normal distribution of basal cells in all genotypes (Figures 2A–2D). Analyses of CCSP demonstrated a normal pattern of columnar cells in WT and rtTA$^+$ mice (Figures 2H and 2I). In contrast, the CCSP$^+$ cells in Cre$^+$ (Figure 2J) and BiTg (Figure 2K) mice were goblet-shaped and appeared to demonstrate increased CCSP staining relative to WT and rtTA mice. An antibody dilution analysis demonstrated that the titer for the supraoptimal detection of CCSP (38, 39) in WT mice was 1 in
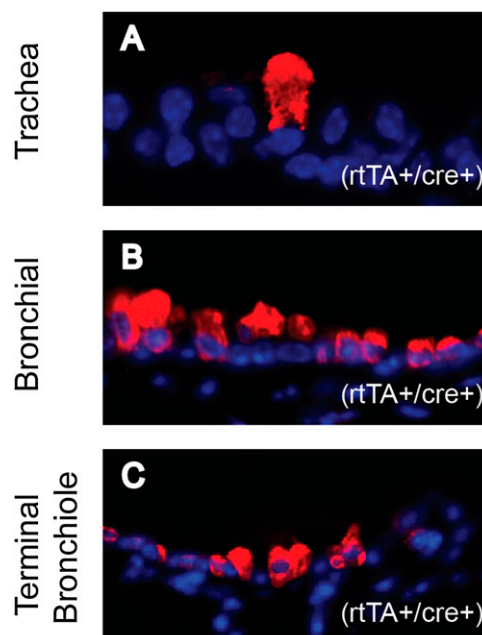

Figure 1. Immunodetection of Clara-cell secretory protein (CCSP) in K14-rtTA$^{+/0}$/TRE-Cre$^{+/0}$/DE3$^{+/+}$ (BiTg) mice. CCSP staining of tracheal (*A*), bronchial (*B*), and terminal bronchiolar (*C*) epithelia. Images are representative of large, highly autofluorescent Clara-type cells. CCSP, *red*; 4′,6-diamidino-2-phenylindole (DAPI), *blue*. K14, keratin 14; rtTA, reverse-tetracycline transactivator; TRE, tetracycline-responsive element; DE3, β-catenin floxed exon 3.

4,000, and 1 in 80,000 for BiTg mice (Figure E1 in the online supplement). These data demonstrate that abnormal CCSP$^+$ cells contained more immunoreactive CCSP protein. The abnormal cells detected in Cre$^+$ and BiTg mice were highly autofluorescent and CCSP$^+$. Periodic acid–Schiff (PAS) staining did not detect glycoconjugate, indicating that these were not mucus cells (not shown). Thus, the abnormal CCSP$^+$ cells were likely to be dying Clara cells. All groups exhibited acetylated tubulin–positive (ACT$^+$) apical cilia (Figures 2H–2K). Analyses of the mitotic index in rtTA and BiTg mice did not detect genotype-dependent alterations in proliferation (Figure E2).

Vv/Sv for tracheal nuclei and cell subtypes. An analysis of total nuclear Vv/Sv demonstrated that the WT nuclear mass was significantly greater than that of BiTg (Figure 2E, $P = 8 \times 10^{-4}$). To determine if this effect was attributable to depletion of a specific cell type, the Vv/Sv for K5$^+$, CCSP$^+$, and ACT$^+$ cells was determined. The Vv/Sv for K5$^+$ cells was approximately threefold greater in WT compared with BiTg mice (Figure 2F, $P = 4 \times 10^{-8}$). As previously demonstrated (32), most tracheal basal cells were K14$^-$ (Figures 2A–2D). Staining of the esophagus served as the positive control for K14 staining (Figures E2A–E2D). Genotype-dependent effects on the K14$^+$ basal-cell subset were not detected (Figure 2K, $P = 0.18$), and indicated that basal cells did not assume the reparative phenotype (32). The Vv/Sv for CCSP$^+$ cells was approximately 12-fold greater for WT compared with BiTg mice (Figure 2L, $P = 7 \times 10^{-5}$). Genotype-dependent effects on the Vv/Sv of ACT$^+$ cells were not detected ($P = 0.08$). This analysis demonstrated a genotype-dependent decrease in tracheal epithelial cell mass, and identified the K5$^+$ basal cell and the CCSP$^+$ Clara-like cell as the affected cell types.

Histological analysis of the intrapulmonary airway. This study evaluated the same animals involved in the tracheal analysis. Immunofluorescence analysis of CCSP detected columnar Clara cells
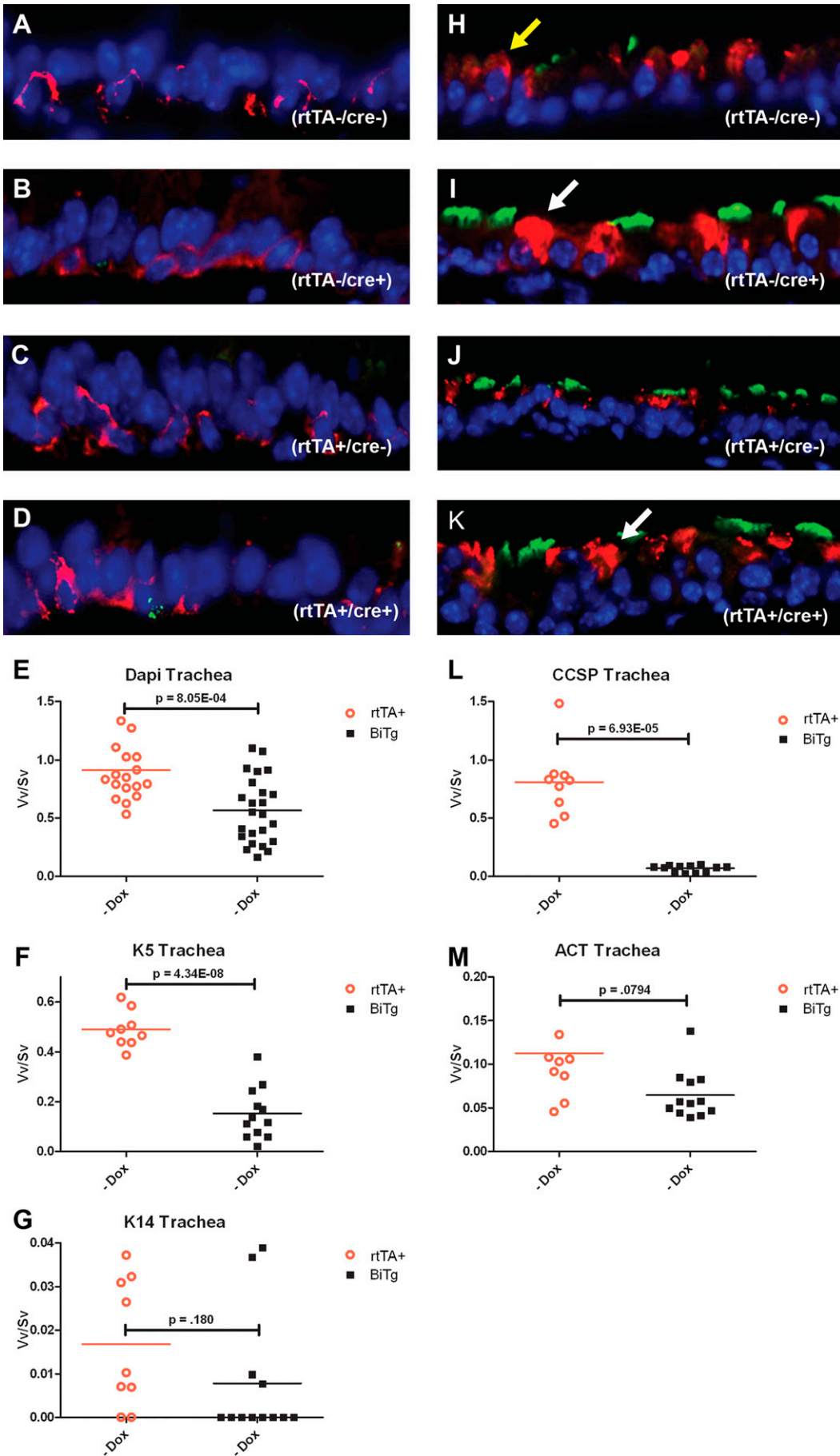
Figure 2. Histological analyses of tracheal epithelia in adult male K14-rtTA/TRE-Cre/DE3 mice of various genotypes receiving standard chow. These genotypes included wild-type (WT) (*A* and *H*), Cre$^+$ (*B* and *I*), rtTA$^+$ (*C* and *J*), and BiTg (*D* and *K*). (*A–D*) Tracheal sections were stained for basal-cell markers K5 and K14 (K5 in *red*, and K14 in *green*). (*H–K*) Tracheal sections were stained for Clara-like and ciliated cell markers CCSP and acetylated tubulin (ACT) (CCSP in *red*, and ACT in *green*). Normal CCSP staining (*yellow arrow*) was evident in WT and rtTA$^+$ genotypes (*H* and *J*), whereas large goblet-shaped CCSP$^+$ cells (*white arrow*) are present in Cre$^+$ and BiTg genotypes (*I* and *K*). (*E, F, L,* and *M*) We performed a morphometric analysis of WT versus BiTg mice receiving standard chow. The nuclear volume density/surface density (Vv/Sv, i.e., total cell mass) was decreased in BiTg (*E*). K5$^+$ cells were decreased approximately threefold in BiTg (*F*), and CCSP$^+$ cells were decreased approximately eightfold in BiTg. No significant difference was evident for K14$^+$ cells (*G*) and ACT$^+$ cells (*M*). Significance was established at $P \leqslant 0.05$. Dox, doxycycline.
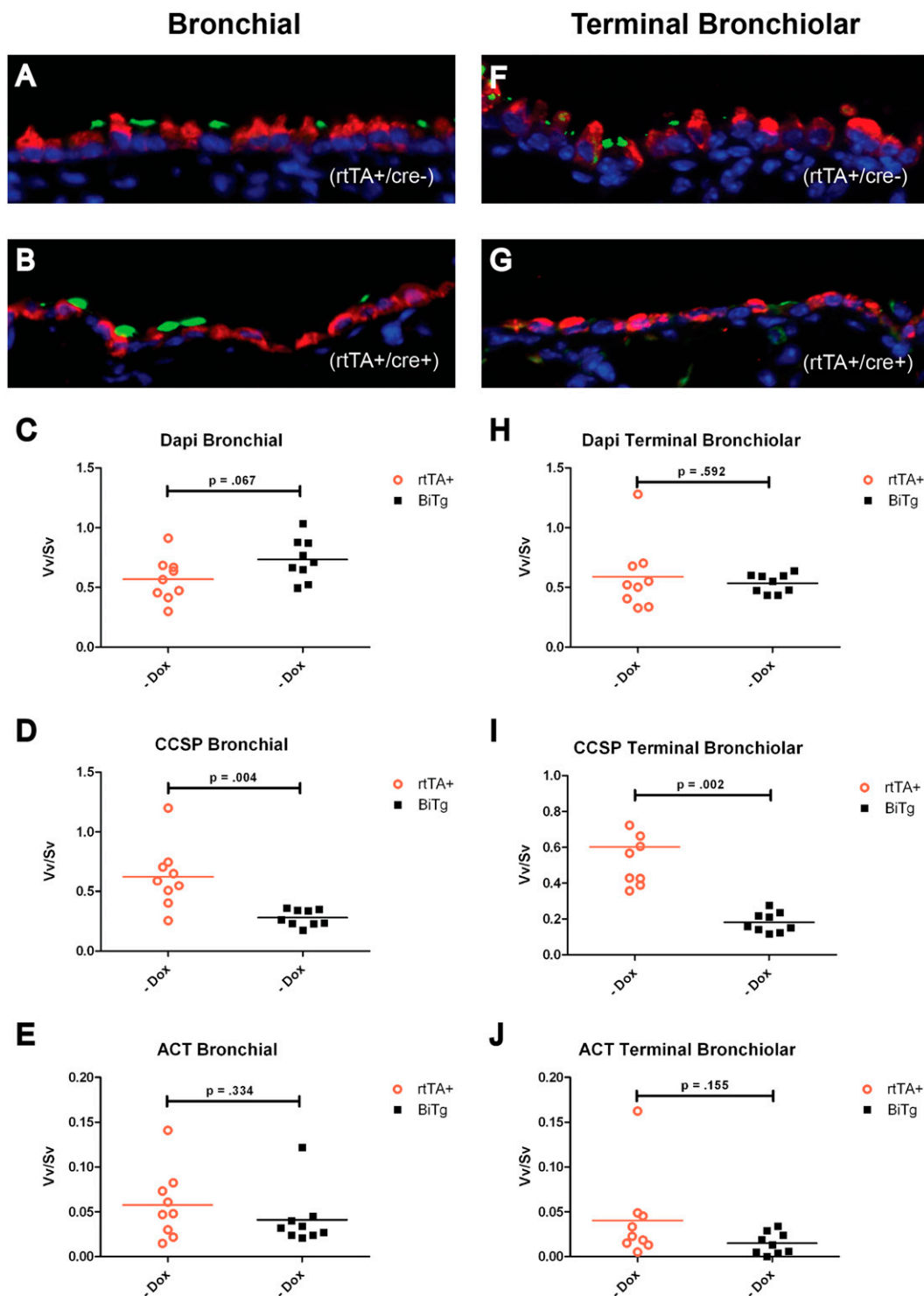
Bronchial

Terminal Bronchiolar

Figure 3. Histological analyses of bronchial and terminal bronchiolar epithelia of rtTA[+] (*A* and *F*) and BiTg (*B* and *G*) mice receiving standard chow. CCSP, *red*; ACT, *green*. We also performed morphometric analyses of WT versus BiTg mice for nuclear mass (*C* and *H*), CCSP (*D* and *I*), and ACT (*E* and *J*). CCSP^{+} cells were decreased approximately twofold in bronchial epithelia (*D*), and approximately fivefold in terminal bronchiolar epithelia (*I*). No genotype-dependent differences were detected for DAPI or ACT. Significance was established at $P \leqslant 0.05$.

in the bronchial (Figures 3A and 3B) and terminal bronchiolar (Figures 3F and 3G) epithelia of WT (not shown) and rtTA[+] mice. In contrast, CCSP^{+} cells in Cre[+] (not shown) and BiTg mice were squamated. PAS staining did not detect glycoconjugate in any genotype (not shown). Analyses of ACT^{+} ciliated cells detected apical cilia in both the bronchial (Figures 3A and 3B) and terminal bronchiolar (Figures 3F and 3G) epithelia.

Bronchial and terminal bronchiolar cell Vv/Sv. The analysis of nuclear Vv/Sv in bronchial epithelia demonstrated that the WT nuclear mass was not different from that of BiTg (Figure 3C, $P =$

0.07). In contrast, the total mass of CCSP^{+} cells was approximately twofold greater in WT compared with BiTg mice (Figure 3D, $P = 0.004$). The Vv/Sv of ACT^{+} cells did not vary by genotype (Figure 3E, $P = 0.33$).

Analyses of nuclear Vv/Sv for the terminal bronchiolar epithelium demonstrated that WT was not different from BiTg (Figure 3H, $P = 0.50$). In contrast, the Vv/Sv of CCSP^{+} cells was approximately fivefold greater in WT compared with BiTg mice (Figure 3I, $P = 0.002$). The Vv/Sv of ACT^{+} cells did not vary by genotype (Figure 3J, $P = 0.16$). This analysis demonstrated that

the bronchiolar epithelial nuclear mass and ciliated cell mass were genotype-independent. However, a genotype-dependent decrease in the CCSP$^+$ Clara-cell mass was also evident.

Mechanism Regulating the Genotype-Dependent Effect

Nuclear Cre protein in the bronchial and terminal bronchial epithelium. The genetic difference between normal (WT and rtTA$^+$) and abnormal (Cre$^+$ and BiTg) tissues was the TRE-Cre transgene. These data suggest a Cre recombinase–dependent effect. To determine if Cre recombinase was expressed in bronchial or bronchiolar epithelia, BiTg mice received standard chow, and their lung tissue was evaluated for Cre protein by immunofluorescence. Nuclear Cre was present in the bronchial (Figure E4A) and terminal bronchiolar (Figure E4B) epithelium. These data demonstrate the expression of the TRE-Cre transgene in the absence of inducer.

Western blot analysis of DE3 allele modification. The detection of Cre protein in BiTg mice receiving standard chow suggested recombination of the DE3 allele. To test this possibility, Western blots were used to evaluate the expression of WT β-catenin and the mutant β-catenin generated by the recombined DE3 allele. Epitope-specific β-catenin antibodies were used to probe tissue homogenates. The specificity of the antibodies was demonstrated by Western blotting (Figure E5).

All tissues used in this analysis were from mice fed standard chow. Tracheal and lung protein from WT or rtTA$^+$ mice expressed only WT β-catenin (Figure 4). In contrast, tracheal or lung tissue from Cre$^+$ or BiTg mice expressed both the WT and DE3 β-catenin. Western blot analysis of esophageal tissue protein, which expressed high concentrations of K14 (32), was used to determine if the DE3 allele was recombined in other tissues. The mutant β-catenin protein was detected in only one of 13 esophagi tested (Figure 4). The only tissue that expressed the mutant β-catenin was BiTg. These data indicate that: (*1*) the DE3 allele was recombined in respiratory epithelia of mice that harbored the TRE-Cre transgene; (*2*) recombination of the DE3 allele was driver-independent and Dox-independent; and (*3*) the floxed β-catenin allele was one target of spurious Cre recombinase activity.

Recombination of the ROSA26-floxed STOP-LacZ allele. To determine the cell-type specificity and extent of Cre-mediated recombination in the trachea and lung, mice harboring one copy of the DE3 allele and one copy of the ROSA26-floxed STOP-LacZ recombination substrate (RS) allele were analyzed. Recombination of the RS allele results in the expression of β-gal, and is detected by X-gal staining.

Recombination was not detected in the trachea of mice that were TRE-Cre transgene–negative (not shown). However, a low level of recombination was detected in tracheas of mice that
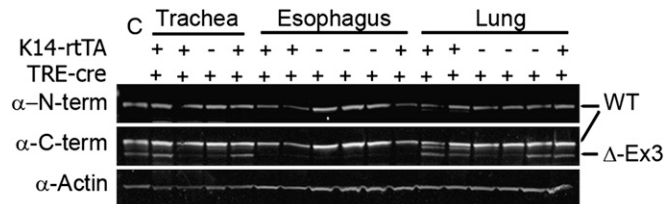

Figure 4. Western blot analysis of WT and DE3 (Δ-Ex3) β-catenin in tracheal, esophageal, and lung protein. Genotype is indicated above each lane. Blots probed with α–N-terminal (α–N-term) β-catenin show the epitope present in the WT β-catenin, but deleted in the DE3 from. Blots probed with α–C-terminal (α-C-term) β-catenin detect both the WT and DE3 forms. Actin was used as the loading control (C). Dual-color detection methods were used, but color-separated monochrome images are presented here.

were TRE-Cre transgene–positive (Figures 5A and 5B). To determine the frequency of RS recombination, approximately nine cartilaginous rings per mouse (27 in total) were evaluated for recombined (X-gal$^+$) cells. No recombined cells were found in 25 of 27 rings (93%; Figure 5A). In contrast, small clusters of recombined cells were detected in two of 27 rings (7%; Figure 5B). Recombination of the RS allele was not detected in the terminal bronchiolar or bronchiolar epithelium (Figures 5C and 5D). The discrepancy between the Western blot data and the RS analysis suggested: (*1*) that the RS allele was not a reliable indicator of recombination; and (*2*) that recombination of the DE3 allele, even at concentrations undetectable by the RS reporter, was sufficient to alter the representation of basal and Clara-type cells.

Activation of the TOPGal β-catenin reporter. To determine if the relationship between genotype and phenotype was attributable to the Cre-mediated recombination of the DE3 allele and a result of activating β-catenin–dependent gene expression, we evaluated mice harboring the TRE-Cre transgene, one copy of the DE3 allele, and one copy of the β-catenin activity reporter transgene TOPgal (36). Activation of the TOPGal reporter results in the expression of β-gal, which is detected by X-gal staining.

Expression of the TOPGal transgene was not detected in the tracheas or lungs of mice that were TRE-Cre transgene–negative (Figure 6A). However, reporter activation was detected in the trachea or lungs of mice that were Cre$^+$ (Figures 6B–6D). Transgene activity was detected throughout the epithelial cell layer in tracheal, bronchial, and terminal bronchiolar epithelia. Activation of the TOPGal transgene was absent in nonepithelial tissue types within the trachea and the lung. These data demonstrate the activation of β-catenin–dependent genes in the tracheal and lung epithelium. Based on these studies, we conclude that the driver-independent and Dox-independent activation of the TRE-Cre transgene results in a recombination of the DE3 allele. The consequence of the increased expression of β-catenin–dependent genes was a decreased mass of basal, Clara-like, and Clara cells.

Effects of Treatment (Exposures to Dox) on Differentiated Cell Vv/Sv

To determine the impact of Dox exposure on cellular phenotype, normal adult male mice received standard chow or Dox chow for 6 days, and the Vv/Sv of various cell types was determined. To aid in the presentation of this analysis, the data for WT and BiTg mice receiving standard chow (Figures 2 and 3) are repeated in Figure 7.

Tracheal cells. The Vv/Sv of K5$^+$ cells was greater in WT mice receiving standard chow versus those receiving Dox chow (Figure 7A, $P = 0.007$). The Vv/Sv for K5$^+$ cells did not differ in BiTg mice receiving standard or Dox chow (Figure 7A, $P = 0.581$). The Vv/Sv of CCSP$^+$ cells was twofold greater in WT mice receiving standard chow versus those receiving Dox chow (Figure 7B, $P = 0.02$). The Vv/Sv for CCSP$^+$ cells was lower in BiTg mice receiving standard chow versus Dox chow (Figure 7B, $P = 0.03$). The Vv/Sv for ciliated cells did not vary as a function of chow type for WT mice (Figure 7C, $P = 0.23$). In contrast, the Vv/Sv for ciliated cells in BiTg mice receiving standard chow was greater than in those receiving Dox chow (Figure 7C, $P = 0.05$).

Bronchial cells. The Vv/Sv of CCSP$^+$ cells in WT (Figure 7D, $P = 0.11$) or BiTg (Figure 7D, $P = 0.81$) mice did not vary according to chow type. Similarly, the Vv/Sv of ACT$^+$ cells in WT (Figure 7E, $P = 0.62$) and BiTg (Figure 7E, $P = 0.40$) mice did not vary by type of chow.

Terminal bronchiolar cells. The Vv/Sv of CCSP$^+$ cells in WT (Figure 7F, $P = 0.83$) or BiTg (Figure 7F, $P = 0.26$) mice did not
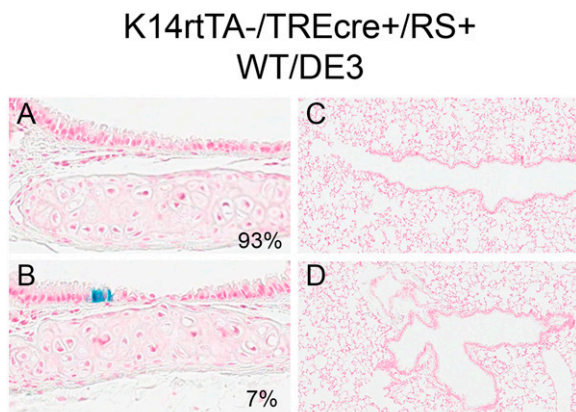
K14rtTA-/TREcre+/RS+
WT/DE3

Figure 5. Aperio imaging of tracheal (*A* and *B*) and lung (*C* and *D*) tissue from K14-rtTA$^{-/-}$/TRE-Cre$^{+/0}$/RS$^{+/0}$/WT/DE3 mice. RS is the ROSA26-floxed recombination substrate transgene. Activity of the β-galactosidase (β-gal) reporter is represented in *blue*. The frequency of the pattern in *A* and *B* is specified in the *lower right corner*.

vary according to chow type. Similarly, the Vv/Sv of ACT$^+$ cells did not vary in WT (Figure 7G, $P = 0.16$) or BiTg (Figure 7G, $P = 0.63$) mice receiving standard or Dox chow. These data indicate that: (*1*) tracheal basal and Clara-like cells are sensitive to Dox exposure; and (*2*) bronchial and bronchiolar Clara cells are not sensitive to Dox exposure.

Interactions between Genotype and Exposures to Dox

A Bonferroni *post hoc* analysis was used to determine whether interactions between genotype and treatment influenced the Vv/Sv of various cell types. This analysis identified genotype as a determinant of the Vv/Sv in tracheal K5$^+$ cells ($P = 0.007$). The interaction between genotype and treatment was not significant. In contrast, the Vv/Sv of tracheal CCSP$^+$ cells was determined primarily by genotype ($P < 0.0001$), and secondarily by exposure to Dox ($P = 0.01$). The interaction between genotype and treatment was significant for tracheal CCSP$^+$ cells ($P = 0.0006$). Interactions between genotype and treatment were not detected among CCSP$^+$ cells in bronchial or terminal bronchiolar epithelia, or among ACT$^+$ cells in any epithelial compartment tested.

DISCUSSION

Summary

We evaluated the impact of genotype and Dox treatment on the cell mass (Vv/Sv) of epithelial cell types in the K14-rtTA/TRE-Cre/DE3 murine strain. We demonstrated that the Vv/Sv of tracheal K5$^+$ basal cells was determined by genotype. In contrast, the Vv/Sv of tracheal CCSP$^+$ cells was determined by genotype and treatment. The Vv/Sv of bronchial and terminal bronchiolar CCSP$^+$ cells was dependent on genotype only. Finally, the Vv/Sv of ACT$^+$ cells was not altered by either genotype or treatment. We attribute the genotype-dependent effects to the spurious activity of the TRE-Cre transgene, recombination of the DE3 β-catenin allele, and activation of β-catenin–dependent gene expression. We also demonstrated that the exposure of WT tracheal K5$^+$ and CCSP$^+$ cells to Dox decreases their Vv/Sv. Beyond the obvious cautionary note regarding the use of Dox-inducible systems to study molecular regulation of tracheal cell-type function, we also report that sensitivity to Dox does not extend to bronchial and terminal bronchiolar Clara cells or ciliated cells. We discuss genotype-dependent alterations in epithelial-cell Vv/Sv in terms of
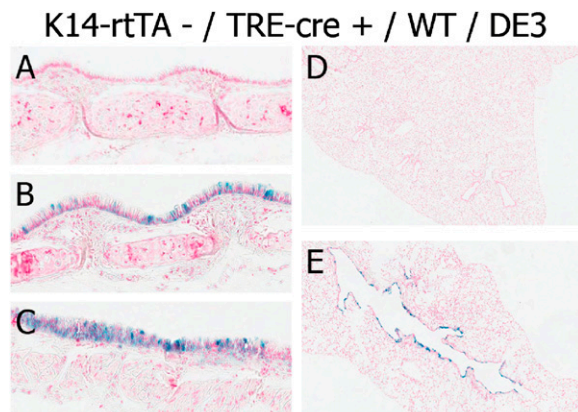
K14-rtTA - / TRE-cre + / WT / DE3

Figure 6. Aperio imaging of tracheal (*A–C*) and lung (*D* and *E*) tissue sections from K14-rtTA$^{-/-}$/TRE-Cre$^{+/0}$/TOPGal$^{+/0}$/WT/DE3 mice. *A* and *D* are TOPGal Tg$^-$, and *B*, *C*, and *E* are TopGal Tg$^+$. β-gal reporter activity is represented in *blue*.

the low-level epithelial damage observed in this model and the β-catenin–dependent alterations in steady-state progenitor cell hierarchies.

Cautionary Notes

Tracheal basal and Clara-like cells are sensitive to Dox. Quantitative histomorphometry demonstrated that treatment with Dox for 6–19 days was toxic, resulting in a significant decrease in the Vv/Sv of WT tracheal basal and Clara-like cells. Importantly, the WT bronchial and terminal bronchiolar Clara-cell Vv/Sv was not altered by exposure to Dox. This differential sensitivity of Clara-type cell subsets to Dox adds to the previously detailed differences between tracheobronchial and intrapulmonary cells (40–42). As previously reported (43, 44), the effects of Dox and distinctions among Clara-type cells should be recognized and controlled for in experiments that use Dox as an inducer of genetic modifications.

Dox is a known inhibitor of matrix metalloproteases (MMPs) and a chelator of divalent cations (43, 45). In models of leukocyte adhesion, these properties antagonize each other by reducing the activity of sheddases (i.e., the inhibition of MMPs) and by decreasing barrier permeability (chelation) (46).

Dox-dependent effects on either the activity of MMPs or barrier function could result in secondary modifications of β-catenin–dependent gene expression. MMPs functioning as sheddases activate various receptor tyrosine kinases (RTKs), which can in turn activate the expression of β-catenin–dependent genes (47–49). Our study cannot address this effect of Dox on control mice, because little to no β-catenin activity was detected in control mice (Figure 6 (50)). Another effect of RTK activation (particularly epidermal growth factor receptor) involves mucus cell metaplasia (51). Although this phenotypic alteration was reported in β-catenin–stabilized models (26), we did not detect PAS-reactive material in this study. Alterations in the epithelial barrier, such as those initiated by chelation, can also lead to the activation of β-catenin–dependent genes (52). This process may account for the Dox-by-genotype interaction detected in tracheal Clara-like cells.

Spurious activity of the TRE-Cre transgene. Detection of nuclear Cre protein in the absence of the Dox inducer (Figure E4) and recombination of the DE3 allele (Figure E5) indicates that the TRE-Cre transgene was not regulated appropriately in this strain. Similar results were obtained in two of the three TRE-Cre lines tested. These lines shared the TRE-Cre allele, but
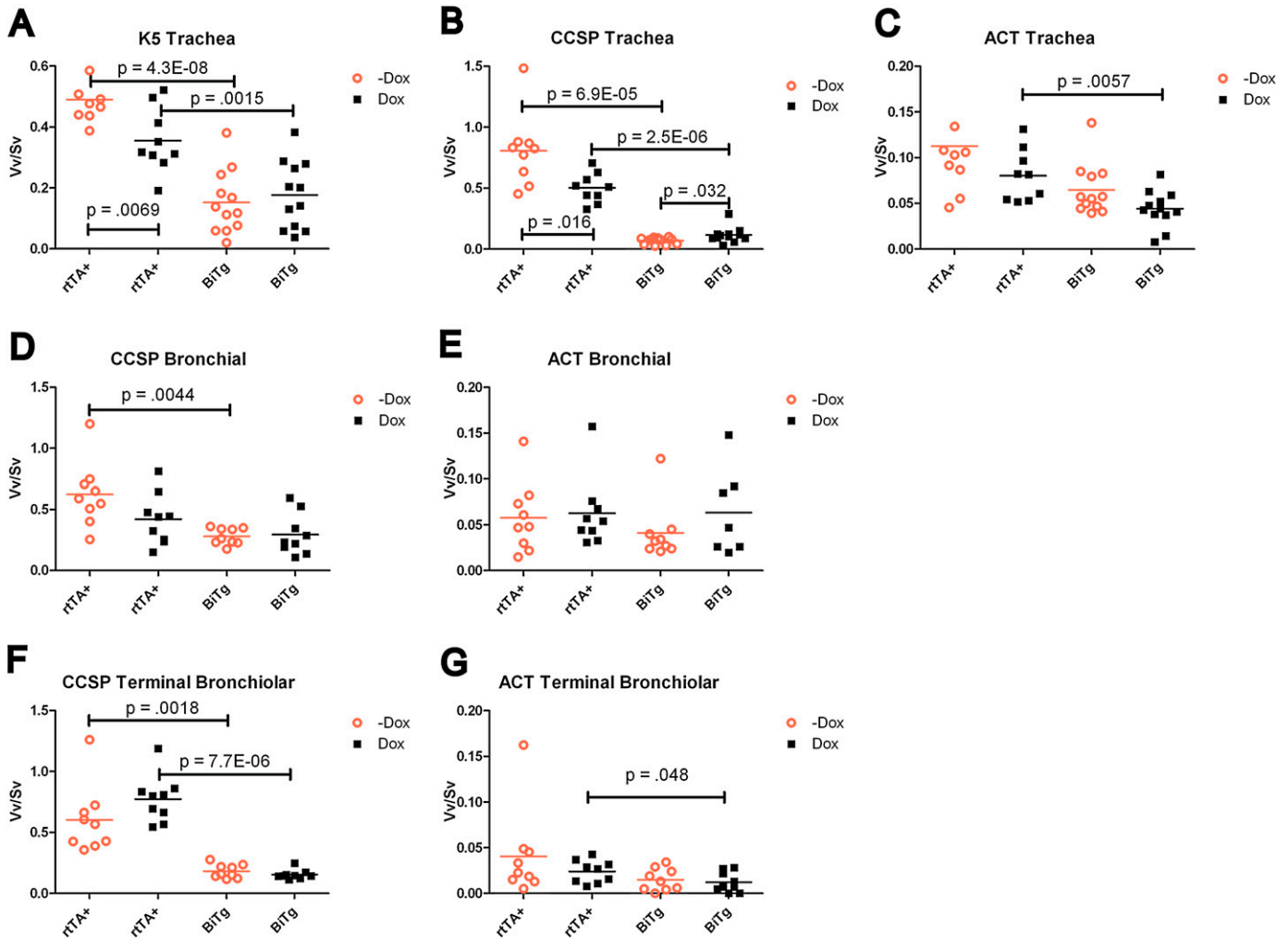
Figure 7. Quantitative histomorphometric analysis of Vv/Sv as a function of genotype and Dox treatment of rtTA$^+$ (K14-rtTA$^+$/TRE-Cre$^-$) and BiTg (K14-rtTA$^+$/TRE-Cre$^-$) mice. Values in graphs represent P values for each pairwise comparison. Significance was established at $P \leq 0.05$.

varied according to the rtTA driver as well as the floxed allele. All mice were a mix of several inbred murine backgrounds. Thus, to determine the cause of spurious Cre activity in some lines but not others would be difficult. These data do indicate that each model system must be rigorously tested for driver-dependence and Dox-dependence. Fortunately, little variation was detected within each line, which overcomes the need for repeated testing.

Reporter transgenes: recombination versus pathway activation. Failure to detect spurious TRE-Cre activity using the RS reporter is of concern (Figure 5). Gain-of-function studies, particularly those focused on β-catenin, frequently use animals that are heterozygous for the DE3 allele (19, 26, 27). Although this approach serves to limit the amount of mutant β-catenin generated, it also prevents immunological identification of cells that have undergone recombination (11). This obstacle is commonly overcome by the analysis of a surrogate allele, the RS (35) or its variants (53). Our data suggest that Cre-mediated recombination is dependent on the concentration of Cre protein. Thus, the ability of the RS to report recombination, particularly when multiple floxed alleles are present, is dependent on the high-level expression of the Cre transgene.

Analysis of β-catenin dosage. We were unable to use epitope-specific β-catenin antibodies (11) to identify cells that had recombined the DE3 allele in BiTg mice (not shown). The failure to detect cells that had undergone recombination in both DE3

alleles is at variance with our previous analysis, which detected numerous bronchiolar cells that were recombined in both DE3 alleles (11). These data suggest two possibilities that may affect interpretations of similar studies. First, the limited recombination of the DE3 allele may be attributable to a survival advantage for cells that retain one WT β-catenin allele. Second, the DE3 protein may initiate a negative feedback loop that alters accessibility of the β-catenin locus to Cre. An investigation of these mechanisms is beyond the scope of the present study.

Roles for β-Catenin–Dependent Gene Injury and Repair

We typically evaluated epithelial repair mechanisms in mice that were challenged with chemical agents such as NA. This model is favored because it increases the mitotic index at least 10-fold, and allows for identification of progenitor cell types and lineage relationships. Although such models are extremely useful, they must be interpreted in the context of extensive epithelial damage and the potential involvement of other cell and tissue types. Consequently, identification of low-level tracheal epithelial damage (i.e., decreased nuclear Vv/Sv) in the BiTg model allowed us the uncommon opportunity to evaluate the roles of β-catenin under conditions of less severe injury, and to compare these results with those in other models of low-level injury (15, 54).

We previously reported that tracheal basal cells were a self-renewing progenitor in the normal trachea (6). After NA injury,

which depletes the tracheal Clara-like/ciliated cell lineage (32), basal cells became precursors to ciliated and Clara-like cells (6). We also used tracheal air–liquid interface cultures to demonstrate that DE3 β-catenin promoted a twofold increase in basal to ciliated cell differentiation, and that DE3 β-catenin blocked basal to Clara-like cell differentiation (50). In the present study, basal and Clara-like cell types were depleted after recombination of the DE3 allele (Figure 3) and activation of β-catenin–dependent gene expression (Figure 5). Despite depletion of the two known ciliated cell progenitors, the Vv/Sv of tracheal ciliated cells was unchanged. Based on our previous analysis of steady-state and post-NA injury lineage relationships, we suggest that the major effect detected in BiTg mice, that is, the genotype-dependent stabilization of β-catenin, altered lineage relationships among tracheal progenitor cells.

We propose the following scenario to explain these results. First, we suggest that the activation of β-catenin–dependent gene expression in Clara-like cells predisposes these cells to death. This conclusion is based on the finding that the surviving Clara-type cells exhibited a goblet-like morphology and were highly autofluorescent. The decrease of Vv/Sv in CCSP$^+$ cells suggested that the enlarged Clara-type cells died. The possibility of an mucus-cell intermediate (55, 56) is diminished because PAS$^+$ cells were not detected, and because Dox is known to antagonize the production of mucus in response to treatment with acrolein in rats (57). Second, we suggest that activation of β-catenin–dependent genes blocked Clara-like to ciliated cell differentiation. This proposal is based on our previous finding that stabilization of β-catenin did not alter the proliferation of Clara cells in response to NA, but did prevent Clara to ciliated cell differentiation (11). Third, we suggest that the activation of β-catenin in tracheal basal cells stimulated basal to ciliated cell differentiation. This proposal is based on our finding that the stabilization of β-catenin increases basal to ciliated cell differentiation in vitro (50). This differentiation pathway likely occurs in the absence of intervening cell division. Thus the proposed mechanism would explain the maintenance of the ciliated cell population as well as the depletion of the basal cell population. Consequently, the ciliated cell population would be maintained at the expense of the basal cell progenitor.

In contrast with the tracheal hierarchy, the bronchiolar ciliated cell is maintained by the Clara cell (8) and its variant, the variant CCSP-expressing cell (58). The present study demonstrates that activation of β-catenin–dependent genes in the absence of overt injury depletes the Clara cell population. We suggest that maintenance of the ciliated cell population is a consequence of the failure by Clara cells to undergo recombination. This finding highlights the importance of the abundant and broadly distributed Clara cell progenitor for the maintenance of bronchiolar and terminal bronchiolar epithelia (9, 59).

References

1. Daniely Y, Liao G, Dixon D, Linnoila RI, Lori A, Randell SH, Oren M, Jetten AM. Critical role of p63 in the development of a normal esophageal and tracheobronchial epithelium. *Am J Physiol Cell Physiol* 2004;287:C171–C181.

2. Evans MJ, Shami SG, Cabral-Anderson LJ, Dekker NP. Role of nonciliated cells in renewal of the bronchial epithelium of rats exposed to NO$_2$. *Am J Pathol* 1986;123:126–133.

3. Ghosh M, Helm KM, Smith RW, Giordanengo MS, Li B, Shen H, Reynolds SD. A single cell functions as a tissue-specific stem cell and the *in vitro* niche-forming cell. *Am J Respir Cell Mol Biol* 2011;45:459–469.

4. Hong KU, Reynolds SD, Watkins S, Fuchs E, Stripp BR. Basal cells are a multipotent progenitor capable of renewing the bronchial epithelium. *Am J Pathol* 2004;164:577–588.

5. Hong KU, Reynolds SD, Watkins S, Fuchs E, Stripp BR. *In vivo* differentiation potential of tracheal basal cells: evidence for multipotent and unipotent subpopulations. *Am J Physiol Lung Cell Mol Physiol* 2004;286:L643–L649.

6. Ghosh M, Brechbuhl HM, Smith RW, Li B, Hicks DA, Titchner T, Runkle CM, Reynolds SD. Context-dependent differentiation of multipotential keratin 14–expressing tracheal basal cells. *Am J Respir Cell Mol Biol* 2011;45:403–410.

7. Rock JR, Onaitis MW, Rawlins EL, Lu Y, Clark CP, Xue Y, Randell SH, Hogan BL. Basal cells as stem cells of the mouse trachea and human airway epithelium. *Proc Natl Acad Sci USA* 2009;106:12771–12775.

8. Evans MJ, Johnson LV, Stephens RJ, Freeman G. Renewal of the terminal bronchiolar epithelium in the rat following exposure to NO$_2$ or O$_3$. *Lab Invest* 1976;35:246–257.

9. Rawlins EL, Okubo T, Xue Y, Brass DM, Auten RL, Hasegawa H, Wang F, Hogan BL. The role of SCGB1A1$^+$ Clara cells in the long-term maintenance and repair of lung airway, but not alveolar, epithelium. *Cell Stem Cell* 2009;4:525–534.

10. Evans MJ, Dekker NP, Cabral-Anderson LJ, Freeman G. Quantitation of damage to the alveolar epithelium by means of Type 2 cell proliferation. *Am Rev Respir Dis* 1978;118:787–790.

11. Reynolds SD, Zemke AC, Giangreco A, Brockway BL, Teisanu RM, Drake JA, Mariani T, Di PY, Taketo MM, Stripp BR. Conditional stabilization of beta-catenin expands the pool of lung stem cells. *Stem Cells* 2008;26:1337–1346.

12. Pinkerton KE, Dodge DE, Cederdahl-Demmler J, Wong VJ, Peake J, Haselton CJ, Mellick PW, Singh G, Plopper CG. Differentiated bronchiolar epithelium in alveolar ducts of rats exposed to ozone for 20 months. *Am J Pathol* 1993;142:947–956.

13. Kim CF, Jackson EL, Woolfenden AE, Lawrence S, Babar I, Vogel S, Crowley D, Bronson RT, Jacks T. Identification of bronchioalveolar stem cells in normal lung and lung cancer. *Cell* 2005;121:823–835.

14. Daly HE, Baecher-Allan CM, Paxhia AT, Ryan RM, Barth RK, Finkelstein JN. Cell-specific gene expression reveals changes in epithelial cell populations after bleomycin treatment. *Lab Invest* 1998;78:393–400.

15. Perl AK, Riethmacher D, Whitsett JA. Conditional depletion of airway progenitor cells induces peribronchiolar fibrosis. *Am J Respir Crit Care Med* 2011;183:511–521.

16. Dean CH, Miller LA, Smith AN, Dufort D, Lang RA, Niswander LA. Canonical WNT signaling negatively regulates branching morphogenesis of the lung and lacrimal gland. *Dev Biol* 2005;286:270–286.

17. Okubo T, Hogan BL. Hyperactive WNT signaling changes the developmental potential of embryonic lung endoderm. *J Biol* 2004;3:11.

18. De Langhe SP, Reynolds SD. WNT signaling in lung organogenesis. *Organogenesis* 2008;4:100–108.

19. Goss AM, Tian Y, Tsukiyama T, Cohen ED, Zhou D, Lu MM, Yamaguchi TP, Morrisey EE. WNT2/2B and beta-catenin signaling are necessary and sufficient to specify lung progenitors in the foregut. *Dev Cell* 2009;17:290–298.

20. Harris-Johnson KS, Domyan ET, Vezina CM, Sun X. Beta-catenin promotes respiratory progenitor identity in mouse foregut. *Proc Natl Acad Sci USA* 2009;106:16287–16292.

21. Harada N, Tamai Y, Ishikawa T, Sauer B, Takaku K, Oshima M, Taketo MM. Intestinal polyposis in mice with a dominant stable mutation of the beta-catenin gene. *EMBO J* 1999;18:5931–5942.

22. Whitsett JA, Perl AK. Conditional control of gene expression in the respiratory epithelium: a cautionary note. *Am J Respir Cell Mol Biol* 2006;34:519–520.

23. Sisson TH, Hansen JM, Shah M, Hanson KE, Du M, Ling T, Simon RH, Christensen PJ. Expression of the reverse tetracycline-transactivator gene causes emphysema-like changes in mice. *Am J Respir Cell Mol Biol* 2006;34:552–560.

24. Morimoto M, Kopan R. RTTA toxicity limits the usefulness of the SP-C-RTTA transgenic mouse. *Dev Biol* 2009;325:171–178.

25. Jeannotte L, Aubin J, Bourque S, Lemieux M, Montaron S, Provencher St.-Pierre A. Unsuspected effects of a lung-specific Cre deleter mouse line. *Genesis* 2011;49:152–159.

26. Mucenski ML, Nation JM, Thitoff AR, Besnard V, Xu Y, Wert SE, Harada N, Taketo MM, Stahlman MT, Whitsett JA. Beta-catenin regulates differentiation of respiratory epithelial cells *in vivo*. *Am J Physiol Lung Cell Mol Physiol* 2005;289:L971–L979.

27. Li C, Li A, Li M, Xing Y, Chen H, Hu L, Tiozzo C, Anderson S, Taketo MM, Minoo P. Stabilized beta-catenin in lung epithelial cells changes cell fate and leads to tracheal and bronchial polyposis. *Dev Biol* 2009;334:97–108.

28. Giangreco A, Reynolds SD, Stripp BR. Terminal bronchioles harbor a unique airway stem cell population that localizes to the bronchoalveolar duct junction. *Am J Pathol* 2002;161:173–182.

29. Reynolds SD, Giangreco A, Power JH, Stripp BR. Neuroepithelial bodies of pulmonary airways serve as a reservoir of progenitor cells capable of epithelial regeneration. *Am J Pathol* 2000;156:269–278.

30. Hyde DM, Plopper CG, Kass PH, Alley JL. Estimation of cell numbers and volumes of bronchiolar epithelium during rabbit lung maturation. *Am J Anat* 1983;167:359–370.

31. Van Winkle LS, Fanucchi MV, Miller LA, Baker GL, Gershwin LJ, Schelegle ES, Hyde DM, Evans MJ, Plopper CG. Epithelial cell distribution and abundance in rhesus monkey airways during postnatal lung growth and development. *J Appl Physiol* 2004;97:2355–2363, discussion 2354.

32. Cole BB, Smith RW, Jenkins KM, Graham BB, Reynolds PR, Reynolds SD. Tracheal basal cells: a facultative progenitor cell pool. *Am J Pathol* 2010;177:362–376.

33. Xie W, Chow LT, Paterson AJ, Chin E, Kudlow JE. Conditional expression of the ERBB2 oncogene elicits reversible hyperplasia in stratified epithelia and up-regulation of TGFalpha expression in transgenic mice. *Oncogene* 1999;18:3593–3607.

34. Perl AK, Wert SE, Nagy A, Lobe CG, Whitsett JA. Early restriction of peripheral and proximal cell lineages during formation of the lung. *Proc Natl Acad Sci USA* 2002;99:10482–10487.

35. Soriano P. Generalized LacZ expression with the ROSA26 Cre reporter strain. *Nat Genet* 1999;21:70–71.

36. DasGupta R, Fuchs E. Multiple roles for activated LEF/TCF transcription complexes during hair follicle development and differentiation. *Development* 1999;126:4557–4568.

37. Hyde DM, Tyler NK, Plopper CG. Morphometry of the respiratory tract: avoiding the sampling, size, orientation, and reference traps. *Toxicol Pathol* 2007;35:41–48.

38. McBride JT, Springall DR, Winter RJ, Polak JM. Quantitative immunocytochemistry shows calcitonin gene–related peptide-like immunoreactivity in lung neuroendocrine cells is increased by chronic hypoxia in the rat. *Am J Respir Cell Mol Biol* 1990;3:587–593.

39. Roncalli M, Springall DR, Maggioni M, Moradoghli-Haftvani A, Winter RJ, Zhao L, Coggi G, Polak JM. Early changes in the calcitonin gene–related peptide (CGRP) content of pulmonary endocrine cells concomitant with vascular remodeling in the hypoxic rat. *Am J Respir Cell Mol Biol* 1993;9:467–474.

40. Plopper CG, Mariassy AT, Hill LH. Ultrastructure of the nonciliated bronchiolar epithelial (Clara) cell of mammalian lung: I. A comparison of rabbit, guinea pig, rat, hamster, and mouse. *Exp Lung Res* 1980;1:139–154.

41. Plopper CG, Mariassy AT, Hill LH. Ultrastructure of the nonciliated bronchiolar epithelial (Clara) cell of mammalian lung: II. A comparison of horse, steer, sheep, dog, and cat. *Exp Lung Res* 1980;1:155–169.

42. Stripp BR, Reynolds SD. Clara cells. In: Shapiro S, Laurent G, editors. Encyclopedia of respiratory medicine. St. Louis, MO: Elsevier; 2006. pp. 471–477.

43. Vieillard-Baron A, Frisdal E, Raffestin B, Baker AH, Eddahibi S, Adnot S, D'Ortho MP. Inhibition of matrix metalloproteinases by lung TIMP-1 gene transfer limits monocrotaline-induced pulmonary vascular remodeling in rats. *Hum Gene Ther* 2003;14:861–869.

44. Ohbayashi H. Matrix metalloproteinases in lung diseases. *Curr Protein Pept Sci* 2002;3:409–421.

45. Roomi MW, Monterrey JC, Kalinovsky T, Niedzwiecki A, Rath M. Modulation of MMP-2 and MMP-9 by cytokines, mitogens and inhibitors in lung cancer and malignant mesothelioma cell lines. *Oncol Rep* 2009;22:1283–1291.

46. Lipowsky HH, Sah R, Lescanic A. Relative roles of doxycycline and cation chelation in endothelial glycan shedding and adhesion of leukocytes. *Am J Physiol Heart Circ Physiol* 2011;300:H415–H422.

47. Kim HH, Sierke SL, Koland JG. Epidermal growth factor–dependent association of phosphatidylinositol 3-kinase with the ERBB3 gene product. *J Biol Chem* 1994;269:24747–24755.

48. Okwueze MI, Cardwell NL, Pollins AC, Nanney LB. Modulation of porcine wound repair with a transfected ERBB3 gene and relevant EGF-like ligands. *J Invest Dermatol* 2007;127:1030–1041.

49. Soltoff SP, Carraway KL III, Prigent SA, Gullick WG, Cantley LC. ERBB3 is involved in activation of phosphatidylinositol 3-kinase by epidermal growth factor. *Mol Cell Biol* 1994;14:3550–3558.

50. Brechbuhl HM, Ghosh M, Smith MK, Smith RW, Li B, Hicks DA, Cole BB, Reynolds PR, Reynolds SD. Beta-catenin dosage is a critical determinant of tracheal basal cell fate determination. *Am J Pathol* 2011;179:367–379.

51. Kim S, Shim JJ, Burgel PR, Ueki IF, Dao-Pick T, Tam DC, Nadel JA. IL-13–induced Clara cell secretory protein expression in airway epithelium: role of EGFR signaling pathway. *Am J Physiol Lung Cell Mol Physiol* 2002;283:L67–L75.

52. Douglas IS, Diaz del Valle F, Winn RA, Voelkel NF. Beta-catenin in the fibroproliferative response to acute lung injury. *Am J Respir Cell Mol Biol* 2006;34:274–285.

53. Que J, Wilm B, Hasegawa H, Wang F, Bader D, Hogan BL. Mesothelium contributes to vascular smooth muscle and mesenchyme during lung development. *Proc Natl Acad Sci USA* 2008;105:16626–16630.

54. Sisson TH, Mendez M, Choi K, Subbotina N, Courey A, Cunningham A, Dave A, Engelhardt JF, Liu X, White ES, *et al.* Targeted injury of Type II alveolar epithelial cells induces pulmonary fibrosis. *Am J Respir Crit Care Med* 2010;181:254–263.

55. Evans CM, Williams OW, Tuvim MJ, Nigam R, Mixides GP, Blackburn MR, DeMayo FJ, Burns AR, Smith C, Reynolds SD, *et al.* Mucin is produced by Clara cells in the proximal airways of antigen-challenged mice. *Am J Respir Cell Mol Biol* 2004;31:382–394.

56. Larson SD, Plopper CG, Baker G, Tarkington BK, Decile KC, Pinkerton K, Mansoor JK, Hyde DM, Schelegle ES. Proximal airway mucous cells of ovalbumin-sensitized and -challenged brown norway rats accumulate the neuropeptide calcitonin gene–related peptide. *Am J Physiol Lung Cell Mol Physiol* 2004;287:L286–L295.

57. Ren S, Guo LL, Yang J, Liu DS, Wang T, Chen L, Chen YJ, Xu D, Feng YL, Wen FQ. Doxycycline attenuates acrolein-induced mucin production, in part by inhibiting MMP-9. *Eur J Pharmacol* 2011;650:418–423.

58. Hong KU, Reynolds SD, Giangreco A, Hurley CM, Stripp BR. Clara cell secretory protein–expressing cells of the airway neuroepithelial body microenvironment include a label-retaining subset and are critical for epithelial renewal after progenitor cell depletion. *Am J Respir Cell Mol Biol* 2001;24:671–681.

59. Van Winkle LS, Buckpitt AR, Nishio SJ, Isaac JM, Plopper CG. Cellular response in naphthalene-induced Clara cell injury and bronchiolar epithelial repair in mice. *Am J Physiol* 1995;269:L800–L818.